

Adaptive-Gain Second Order Sliding Mode Observer Design for Switching Power Converters

Jianxing Liu, Salah Laghrouche, M.Harmouche and Maxime Wack
Laboratoire IRTES, Université de Technologie de Belfort-Montbéliard,
Belfort, France.

jiang-xing.Liu@utbm.fr; salah.laghrouche@utbm.fr;
mohamed.harmouche@utbm.fr; maxime.wack@utbm.fr

Abstract

In this paper, a novel adaptive-gain Second Order Sliding Mode (SOSM) observer is proposed for multicell converters by considering it as a class of hybrid systems. The aim is to reduce the number of voltage sensors by estimating the capacitor voltages only from the measurement of load current. The proposed observer is proven to be robust in the presence of perturbations with *unknown* boundary. However, the states of the system are only partially observable in the sense of observability rank condition. Due to its switching behavior, a recent concept of $\mathcal{Z}(T_N)$ observability is used to analysis its hybrid observability, since its observability depends upon the switching control signals. Under certain condition of the switching sequences, the voltage across each capacitor becomes observable. Simulation results and comparisons with Luenberger switched observer highlight the effectiveness and robustness of the proposed observer with respect to output measurement noise and system uncertainties (load variations).

Index Terms

sliding mode observer; hybrid systems; observability; multicell power converter

I. INTRODUCTION

In recently years, industrial applications require high power level by using medium-voltage semiconductors [1], [2], [3], [4]. Due to the efficiency requirements, the power of the converter is generally increased by boosting the voltage. However, medium-voltage switching devices are not available, even if it exists, it will result in large volume and high price [5]. In this sense, the topology of multilevel converter which has been studied during the last decade become attractive to high voltage applications [1]. This structure possesses the possibility of reducing the voltage constraints evenly among each cell in series. These lower voltage switches result in lower conduction losses and higher

switching frequencies. Moreover, it makes possible to improve the output waveforms [5]. These flying capacitors have to be balanced to guarantee the desired voltage values at the output in order to benefit as much as possible from the large potential of the multicell structure [6]. Due to the fact that these properties will be lost if the capacitor voltage drifts far from the desired value [7]. Therefore, a suitable control of switches is needed to generate the desired values of the capacitor voltages. Such control of switches allows to cancel the current harmonics at the cutting frequency and to reduce the ripple of the chopped voltage [8], [9].

Several control methods have been proposed for the multicell converters, such as nonlinear control based on input-output linearization [5], predictive control [10], hybrid control [11], model predictive control [10], [12], sliding mode control [8], [13], [14]. However, most of the above works require the measurements of the voltages of capacitors to design the control. That is, it needs extra voltage sensors which increases the cost and complexity of the system. Hence, the estimation of capacitor voltages by using an observer attracts great interest [15].

Notice that the states of the multicell system are only partially observable since the observability matrix never has full rank [15]. Hence, the results obtained from matrix rank condition for observability analysis of the hybrid systems can not be employed in our system [16], [17]. A recent concept of $Z(T_N)$ -observability [18] for the switched hybrid system is used to analysis its observability, since its observability depends upon the switching control signals. Different observers have been designed for the multicell converters based on such concept, for instance, homogeneous finite time observer [9], super-twisting sliding mode observer [7], [19] and adaptive observer [7]. This concept in [18] gives the condition that under which there exists a hybrid time trajectory that makes the system observable. Then, the estimates of the capacitor voltages can be obtained from the measurements of the load current and source voltage by taking advantage of appropriate hybrid time trajectories, by means of calculating the inverse of a matrix whose elements are those hybrid switching sequences with the assumption that the capacitor voltage is continuous without any jump [7], [9].

In this paper, Firstly, observability analysis of the multicell converter from the measurements of the load current and source voltage under certain conditions of the switching input sequences is done based on the result of [18]. Based on these conditions, the continuous states of the system become observable in the sense of $Z(T_N)$ -observability. Secondly, a novel adaptive-gain SOSM observer for the multi-cell converters has been proposed by taking into account some perturbations (load variations) with the boundary of its first time derivative *unknown*. The proposed adaptive SOSM algorithm combines the nonlinear term of super-twisting algorithm and linear term, so-called SOSML algorithm [20]. The behavior of SOSM around the origin is very strong compared to the linear case. On the other side, the additional linear term improves the behavior of SOSM algorithms far from the origin. Therefore, the SOSML algorithm inherits the

best properties of both the linear and the nonlinear terms. An adaptive law of the gains of the SOSML algorithm is designed via so-called 'time scaling' approach [21]. The output observation error and its first time derivative converge to zero in finite time with the proposed SOSML observer, such that the equivalent output-error injection can be obtained directly. Finally, the resulting reduced order system is proven to be exponential stable. That is, the observer error of the capacitor voltages which are considered as the states of the observer system converge to zero exponentially. The main advantages of the proposed adaptive-gain SOSML are that : Only one parameter needs to be tuned and there is no need a-priori requirement of the perturbation bounds.

This paper has been organized as follows. In Section II, the model of multi-cell converter and its characteristics are presented. In Section III, the observability of multicell converter is studied with the concept of $Z(T_N)$ -observability. Section IV is devoted to the design of the proposed adaptive-gain SOSML observer for estimating the capacitor voltages. Section V gives simulations results compared with Luenberger switched observer under disturbance condition.

II. MODELING OF MULTICELL CONVERTER

Multicell converter is based on the association of a certain number of cells, which consists of an energy storage element and commutators [5]. The main advantage of this structure is that the spectral quality of the output signal is improved by a high switching frequency between the intermediate voltage levels [22]. An instantaneous model which describes fully the hybrid behavior of the multicell converter is considered in our paper [5].

Figure 1 depicts the topology of a converter with p independent commutation cells, connected to an inductive load. The current I flows from the source E to the output through different converter switches. It has a hybrid behavior due to discrete variables (switching logic) and continuous variables (currents and voltages).

Through the circuit analysis, the dynamics of the p-cells converter are presented as the following differential equations,

$$\left\{ \begin{array}{l} \dot{I} = -\frac{R}{L}I + \frac{E}{L}S_p - \sum_{j=1}^{p-1} \frac{V_{c_j}}{L}(S_{j+1} - S_j), \\ \dot{V}_{c_1} = \frac{I}{c_1}(S_2 - S_1), \\ \vdots \\ \dot{V}_{c_{p-1}} = \frac{I}{c_p}(S_p - S_{p-1}). \end{array} \right. \quad (1)$$

where I is the load current, c_j is the j^{th} capacitor, V_{c_j} is the voltage of the j^{th} capacitor, and E is the voltage of the source. Each commutation cell is controlled by the binary input signal $S_j \in \{0, 1\}$. $S_j = 1$ means that the upper switch of the j th cell is on and the lower switch is off, whereas $S_j = 0$ means that the upper switch is off and the lower switch is on. The discrete inputs are defined as follows,

$$\begin{cases} u_j = S_{j+1} - S_j, & j = 1, \dots, p-1 \\ u_p = S_p. \end{cases} \quad (2)$$

With equation (2), the system (1) can be represented as follows

$$\begin{cases} \dot{I} = -\frac{R}{L}I + \frac{E}{L}u_p - \sum_{j=1}^{p-1} \frac{V_{c_j}}{L}u_j, \\ \dot{V}_{c_1} = \frac{I}{c_1}u_1, \\ \vdots \\ \dot{V}_{c_{p-1}} = \frac{I}{c_{p-1}}u_{p-1}, \\ y = I. \end{cases} \quad (3)$$

Assume that only the load current I can be measured, it is easy to present the system (3) as a hybrid (switched affine) system

$$\begin{cases} \dot{x} = f(x, u) = A(u)x + B(u), \\ y = h(x, u) = Cx. \end{cases} \quad (4)$$

where $x = [I \ V_{c_1} \ \dots \ V_{c_{p-1}}]^T$ is the continuous state, $u = [u_1 \ u_2 \ \dots \ u_p]^T$ is the switching control signal which takes only discrete values, and the vectors $A(u)$, $B(u)$, C are defined as

$$\begin{aligned} A(u) &= \begin{bmatrix} -\frac{R}{L} & -\frac{u_1}{L} & \dots & -\frac{u_{p-1}}{L} \\ \frac{u_1}{c_1} & 0 & \dots & 0 \\ \vdots & \vdots & \ddots & \vdots \\ \frac{u_{p-1}}{c_{p-1}} & 0 & \dots & 0 \end{bmatrix}, \\ B(u) &= \begin{bmatrix} \frac{E}{L}u_p & 0 & \dots & 0 \end{bmatrix}^T, \\ C &= [1 \ 0 \ \dots \ 0]. \end{aligned} \quad (5)$$

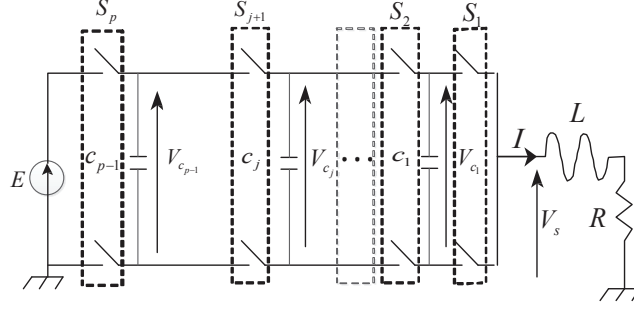


Fig. 1. Multicell converter on RL load

The main object of this paper is that, based on the instantaneous model (3), design an observer which is able to estimate the capacitor voltages only from the measurement of load current and associated switching control input (it is assumed to be known).

III. HYBRID OBSERVABILITY ANALYSIS

Considering the instantaneous model of the system (4) with $p \geq 3$, it can be seen that there are several operating switching modes which make the system unobservable. For instance, if $u_1 = u_2 = \dots = u_{p-1} = 0$, the voltages $V_{c_j} (j = 1, \dots, p-1)$ become completely unobservable. These operating switching modes are not affected by the capacitor voltages. Fortunately, these cases mean that the p-cells are not switching, and will not occur for all control sequences, otherwise there is no interest in physical sense.

The observability analysis of the system (4) is based on the measurement of the load current I and the knowledge of the control input sequence u . The so-called observability matrix [15] is defined as,

$$\mathcal{O}_{p \times p} = \begin{bmatrix} C \\ CA \\ CA^2 \\ \vdots \\ CA^{p-1} \end{bmatrix} = \begin{bmatrix} 1 & 0 & \dots & 0 \\ -\frac{R}{L} & -\frac{u_1}{L} & \dots & -\frac{u_{p-1}}{L} \\ (\frac{R}{L})^2 - \sum_{i=1}^{p-1} \frac{u_i^2}{Lc_i} & \frac{Ru_1}{L^2} & \dots & \frac{Ru_{p-1}}{L^2} \\ \vdots & \vdots & \vdots & \vdots \end{bmatrix}. \quad (6)$$

With simple computation,

$$\text{rank}(\mathcal{O}) = 2 < p. \quad (7)$$

It follows that continuous states are not observable only from the load current in the sense that the rank condition (7) of the observability matrix is not satisfied.

Due to the hybrid behavior of the systems (4), its observability is strongly linked to the hybrid switching sequences. Therefore, a recent $Z(T_N)$ observability concept [18] is applied to analyze the hybrid observability of the systems (4). It is important to give the following definitions.

Definition 1. [18] A hybrid time trajectory is a finite or infinite sequence of intervals $T_N = \Gamma_{i=0}^N$, such that

- $\Gamma_i = [t_{i,0}, t_{i,1})$, for all $0 \leq i < N$;
- For all $i < N$, $t_{i,1} = t_{i+1,0}$;
- $t_{0,0} = t_{ini}$ and $t_{N,1} = t_{end}$.

Moreover, $\langle T_N \rangle$ is defined as the ordered list of u associated to T_N , $u^i_{i=0,N}$ where u^i is the value of u on the interval Γ_i .

Definition 2. [18] The function $z = Z(t, x)$ is said to be Z -Observable with respect to the hybrid time trajectory T_N and $\langle T_N \rangle$, if for all any two trajectories, (t, x, u) and (t, x', u') defined in $[t_{ini}, t_{end}]$, the identity $h(x, u) = h(x', u')$, implies $Z(t, x) = Z(t, x')$.

Lemma 1. [18] Consider the system (4) and a fixed hybrid time trajectory T_N and $\langle T_N \rangle$. Suppose that $z = Z(t, x)$ is always continuous under any admissible control input. If there exists a sequence of projections P_i , $i = 0, 1, \dots, N$, such that

- For all $i < N$, $P_i Z(t, x)$ is Z -Observable for $t \in \Gamma_i$;
- $\text{Rank}([P_0^T, \dots, P_N^T]) = \dim(z)$;
- $\frac{d\bar{P}_i Z(t, x)}{dt} = 0$, for $t \in \Gamma_i$ where \bar{P} is the complement of P (projecting z to the variables eliminated by P).

Then, $z = Z(t, x)$ is Z -observable with respect to the hybrid time trajectory T_N and $\langle T_N \rangle$.

Proof: The proof of the Lemma 1 can be found in [18]. ■

Remark 1. In the Lemma 1, the third condition requires that the components of Z which are not observable in Γ_i must remain constant within this time interval. The hybrid time trajectory T_N and $\langle T_N \rangle$ has their influence on the observability property in the way similar to an input.

Table I presents the eight possible configurations for the three-cell converter. The application of Lemma 1 to the three-cell converter is shown as follows. We take $Z(t, x) = [x_2 \ x_3]^T = [V_{c1} \ V_{c2}]^T$. Under the discrete status $[0, 0, 0]$ and $[1, 1, 1]$, it can be verified that $Z(t, x)$ is not $Z(T_N)$ -observable. Fortunately, from (1), the dynamics of V_{c1}, V_{c2} are zero, which means that the states V_{c1}, V_{c2} keep constant during these time intervals. Then, if a trajectory of the system satisfies that the status is $[1, 0, 0]$ and $[1, 1, 0]$ during time interval Γ_1 and Γ_2 respectively. Let us define $P_1 = [1 \ 0]$, and $P_2 = [0 \ 1]$, obviously,

we have $\bar{P}_1 Z = x_3 = V_{c_2}$, $\frac{d\bar{P}_1 Z}{dt} = \frac{dV_{c_2}}{dt} = 0$, $\bar{P}_2 Z = x_2 = V_{c_1}$, $\frac{d\bar{P}_2 Z}{dt} = \frac{dV_{c_1}}{dt} = 0$ and $\text{rank} \begin{bmatrix} P_1 \\ P_2 \end{bmatrix} = 2$. All the assumptions in the Lemma 1 are satisfied, therefore, $Z(t, x) = \begin{bmatrix} V_{c_1} & V_{c_2} \end{bmatrix}^T$ is $Z(T_N)$ -observable.

TABLE I
DIFFERENT MODES AND CAPACITOR VOLTAGES TENDENCY ASSOCIATED TO A THREE-CELL CONVERTER

Mode : $[S_1, S_2, S_3]$	V_{c_1}	V_{c_2}	u_1	u_2	Observable States
0 : [0,0,0]	\rightsquigarrow	\rightsquigarrow	0	0	I
1 : [0,0,1]	\rightsquigarrow	\nearrow	0	1	I, V_{c_2}
2 : [0,1,0]	\nearrow	\searrow	1	-1	I, V_{c_1}, V_{c_2}
3 : [0,1,1]	\nearrow	\rightsquigarrow	1	0	I, V_{c_1}
4 : [1,0,0]	\searrow	\rightsquigarrow	-1	0	I, V_{c_1}
5 : [1,0,1]	\searrow	\nearrow	-1	1	I, V_{c_1}, V_{c_2}
6 : [1,1,0]	\rightsquigarrow	\searrow	0	-1	I, V_{c_2}
7 : [1,1,1]	\rightsquigarrow	\rightsquigarrow	0	0	I

The symbols in the Table I \rightsquigarrow means keeping constant, \nearrow means increasing and \searrow means decreasing.

In the next Section, an adaptive-gain SOSML observer will be proposed for the system (3).

IV. ADAPTIVE-GAIN SOSML OBSERVER DESIGN

As discussed in [5], active control of the multicell converter requires the knowledge of capacitor voltages. Usually, voltage sensors are used to measure the capacitor voltages. However, the extra sensors increase the cost, complexity and size especially in high voltage applications. Moreover, the sensors are sensitive to high measurement noise since any perturbation on the measurement is directly transposed to the estimated value. Therefore, the design of a state observer only using the measurement of load current and associated switching inputs is an interesting solution.

In this section, an adaptive-gain SOSML observer is proposed for the three-cell converter ($p = 3$) by taking into account some perturbations (load variations) with the boundary of its first time derivative *unknown*. A novel adaptive law of the gains of the SOSML algorithm is designed with only one tuning parameter via so-called 'time scaling' approach [21]. The proposed approach does not require the a-priori knowledge of perturbation bounds.

Define $e_1 = I - \hat{I}$, rewrite the system (3) by taking into account the perturbations

$\tilde{f}(e_1)$ i.e. load resistance uncertainties [9],

$$\begin{cases} \dot{I} = -\frac{R}{L}I + \frac{E}{L}u_3 - \frac{V_{c_1}}{L}u_1 - \frac{V_{c_2}}{L}u_2 + \tilde{f}(e_1), \\ \dot{V}_{c_1} = \frac{u_1}{c_1}I, \\ \dot{V}_{c_2} = \frac{u_2}{c_2}I. \end{cases} \quad (8)$$

The proposed observer is formulated as,

$$\begin{cases} \dot{\hat{I}} = -\frac{R}{L}\hat{I} + \frac{E}{L}u_3 - \frac{\hat{V}_{c_1}}{L}u_1 - \frac{\hat{V}_{c_2}}{L}u_2 + \mu(e_1), \\ \dot{\hat{V}}_{c_1} = \frac{u_1}{c_1}\hat{I} + k_1\mu(e_1), \\ \dot{\hat{V}}_{c_2} = \frac{u_2}{c_2}\hat{I} + k_2\mu(e_1). \end{cases} \quad (9)$$

where $\mu(\cdot)$ is the SOSML algorithm,

$$\mu(e_1) = \lambda(t)|e_1|^{\frac{1}{2}}\text{sign}(e_1) + \alpha(t) \int_0^t \text{sign}(e_1)d\tau + k_\lambda(t)e_1 + k_\alpha(t) \int_0^t e_1d\tau, \quad (10)$$

the adaptive gains $\lambda(t), \alpha(t), k_\lambda(t), k_\alpha(t)$ and designing parameters k_1, k_2 are to be defined.

Define the observation errors as,

$$\begin{cases} e_2 = V_{c_1} - \hat{V}_{c_1}, \\ e_3 = V_{c_2} - \hat{V}_{c_2}. \end{cases} \quad (11)$$

Equations (8) and (9) yield the observation error dynamics as,

$$\dot{e}_1 = -\mu(e_1) - \frac{u_1}{L}e_2 - \frac{u_2}{L}e_3 + \tilde{f}(e_1), \quad (12)$$

$$\dot{e}_2 = -k_1\mu(e_1), \quad (13)$$

$$\dot{e}_3 = -k_2\mu(e_1). \quad (14)$$

In this paper, the adaptive gains $\lambda(t), \alpha(t), k_\lambda(t), k_\alpha(t)$ are formulated as,

$$\begin{cases} \lambda(t) = \lambda_0\sqrt{l(t)}, \\ \alpha(t) = \alpha_0l(t), \\ k_\lambda(t) = k_{\lambda_0}l(t), \\ k_\alpha(t) = k_{\alpha_0}l^2(t). \end{cases} \quad (15)$$

where $\lambda_0, \alpha_0, k_{\lambda_0}, k_{\alpha_0}$ are some positive constants to be defined and $l(t)$ is a positive time varying scalar function.

The adaptive law of the varying function $l(t)$ and the designing parameters k_1, k_2 are given by,

$$\dot{l}(t) = \begin{cases} k, & \text{if } |e_1| \neq 0 \\ 0, & \text{else} \end{cases} \quad (16)$$

$$k_1 = \begin{cases} -\kappa u_1, & \text{if } |e_1| = 0 \\ 0, & \text{else} \end{cases}, \quad k_2 = \begin{cases} -\kappa u_2, & \text{if } |e_1| = 0 \\ 0, & \text{else} \end{cases} \quad (17)$$

where k , the initial value $l(0)$ and κ are positive constants.

Assumption 1. The system (8) and observer system (9) are bounded input bounded state (BIBS), since a physical system is considered [23].

Assumption 2. There is T_N such that $z = x = [I \ V_{c1} \ V_{c2}]^T$ is Z-observable under the condition of Lemma 1 [9].

Theorem 1. Consider the error system (12) under the Assumptions (1,2). Assume that the perturbation $\tilde{f}(e_1)$ satisfies the following condition,

$$\left| \dot{\tilde{f}}(e_1) \right| \leq \chi_1, \quad \text{and} \quad \tilde{f}(0) = 0, \quad (18)$$

where χ_1 is an **unknown** positive constant. Then, the trajectories of the error system (12) converge to zero in finite time with the adaptive gains (15,16) satisfy the following condition,

$$4\alpha_0 k_{\alpha_0} > 8k_{\lambda_0}^2 \alpha_0 + 9\lambda_0^2 k_{\lambda_0}^2, \quad (19)$$

Proof: The system (12) can be rewritten as,

$$\begin{cases} \dot{e}_1 = -\lambda(t)|e_1|^{\frac{1}{2}}\text{sign}(e_1) - k_\lambda(t)e_1 + \varphi_1, \\ \dot{\varphi}_1 = -\alpha(t)\text{sign}(e_1) - k_\alpha(t)e_1 + \varrho_1. \end{cases} \quad (20)$$

where $\varrho_1 = \left(\dot{\tilde{f}}(e_1) - \frac{u_1}{L}\dot{e}_2 - \frac{u_2}{L}\dot{e}_3 \right)$.

Based on the Assumption 1, as the input u is bounded the state does not go infinity in finite time. Moreover if \hat{I} is bounded all the states of the observer are also bounded during finite time. Consequently, the observation error e_1 is also bounded [23]. It follows from (13, 14) that \dot{e}_2, \dot{e}_3 are bounded which satisfy $|\dot{e}_2| \leq \chi_2$ and $|\dot{e}_3| \leq \chi_3$, where χ_2, χ_3 are some unknown positive values. With equation (18), it is easy to deduce that $|\varrho_1| \leq \chi_1 + \frac{\chi_2}{L} + \frac{\chi_3}{L} = F$, F is an unknown positive value.

A new state vector is introduced in order to present system (20) in a more convenient form for Lyapunov analysis.

$$\zeta = \begin{bmatrix} \zeta_1 \\ \zeta_2 \\ \zeta_3 \end{bmatrix} = \begin{bmatrix} l^{\frac{1}{2}}(t)|e_1|^{\frac{1}{2}}\text{sign}(e_1) \\ l(t)e_1 \\ \varphi_1 \end{bmatrix} \quad (21)$$

and system (20) can be rewritten as,

$$\dot{\zeta} = \frac{l(t)}{|\zeta_1|} \underbrace{\begin{bmatrix} -\frac{\lambda_0}{2} & 0 & \frac{1}{2} \\ 0 & -\lambda_0 & 0 \\ -\alpha_0 & 0 & 0 \end{bmatrix}}_{A_1} \zeta + l(t) \underbrace{\begin{bmatrix} -\frac{k_{\lambda_0}}{2} & 0 & 0 \\ 0 & -k_{\lambda_0} & 1 \\ 0 & -k_{\alpha_0} & 0 \end{bmatrix}}_{A_2} \zeta + \begin{bmatrix} \frac{\dot{l}}{2l(t)}\zeta_1 \\ \frac{\dot{l}}{2l(t)}\zeta_2 \\ \varrho_1 \end{bmatrix}, \quad (22)$$

Then, the following Lyapunov function candidate is introduced for the system (22),

$$V(\zeta) = \zeta^T P \zeta, \quad P = \frac{1}{2} \begin{bmatrix} 4\alpha_0 + \lambda_0^2 & \lambda_0 k_{\lambda_0} & -\lambda_0 \\ \lambda_0 k_{\lambda_0} & 2k_{\alpha_0} k_{\lambda_0}^2 & -k_{\lambda_0} \\ -\lambda_0 & -k_{\lambda_0} & 2 \end{bmatrix}. \quad (23)$$

Taking the derivative of (23) along the trajectories of (22),

$$\dot{V} = -\frac{l(t)}{|\zeta_1|} \zeta^T \Omega_1 \zeta - l(t) \zeta^T \Omega_2 \zeta + \varrho_1 q_1 \zeta + \frac{\dot{l}}{l(t)} q_2 P \zeta, \quad (24)$$

where $q_1 = [-\lambda_0 \quad -k_{\lambda_0} \quad 2]$, $q_2 = [\zeta_1 \quad \zeta_2 \quad 0]$, and

$$\begin{aligned} \Omega_1 &= \frac{\lambda_0}{2} \begin{bmatrix} \lambda_0^2 + 2\alpha_0 & 0 & -\lambda_0 \\ 0 & 2k_{\alpha_0} + 5k_{\lambda_0}^2 & -3k_{\lambda_0} \\ -\lambda_0 & -3k_{\lambda_0} & 1 \end{bmatrix}, \\ \Omega_2 &= k_{\lambda_0} \begin{bmatrix} \alpha_0 + 2\lambda_0^2 & 0 & 0 \\ 0 & k_{\alpha_0} + k_{\lambda_0}^2 & -k_{\lambda_0} \\ 0 & -k_{\lambda_0} & 1 \end{bmatrix}, \end{aligned} \quad (25)$$

It is easy to verify that Ω_1, Ω_2 are positive definite matrices under the condition (19).

Since $\lambda_{\min}(P)\|\zeta\|^2 \leq V \leq \lambda_{\max}(P)\|\zeta\|^2$, Equation (24) can be rewritten as,

$$\dot{V} \leq -l(t) \frac{\lambda_{\min}(\Omega_1)}{\lambda_{\max}^{\frac{1}{2}}(P)} V^{\frac{1}{2}} - l(t) \frac{\lambda_{\min}(\Omega_2)}{\lambda_{\max}(P)} V + \frac{F\|q_1\|_2}{\lambda_{\min}^{\frac{1}{2}}(P)} V^{\frac{1}{2}} + \frac{\dot{l}}{2l(t)} \Delta \Omega \quad (26)$$

where

$$\Delta\Omega = ((4\alpha_0 + \lambda_0^2)\zeta_1^2 + 2\lambda_0 k_{\lambda_0} \zeta_1 \zeta_2 + 2k_{\alpha_0} k_{\lambda_0}^2 \zeta_2^2 - \lambda_0 \zeta_1 \zeta_3 - k_{\lambda_0} \zeta_2 \zeta_3) \leq \zeta^T Q \zeta,$$

$$Q = \begin{bmatrix} 4\alpha_0 + \lambda_0^2 + \lambda_0 k_{\lambda_0} + \frac{\lambda_0}{2} & 0 & 0 \\ 0 & 2k_{\alpha_0} k_{\lambda_0}^2 + \lambda_0 k_{\lambda_0} + \frac{k_{\lambda_0}}{2} & 0 \\ 0 & 0 & \frac{\lambda_0 + k_{\lambda_0}}{2} \end{bmatrix}, \quad (27)$$

With (27), equation (26) becomes,

$$\dot{V} \leq - \left(l(t) \frac{\lambda_{\min}(\Omega_1)}{\lambda_{\max}^{\frac{1}{2}}(P)} - \frac{F\|q_1\|_2}{\lambda_{\min}^{\frac{1}{2}}(P)} \right) V^{\frac{1}{2}} - \left(l(t) \frac{\lambda_{\min}(\Omega_2)}{\lambda_{\max}(P)} - \frac{\dot{l}}{2l(t)} \frac{\lambda_{\max}(Q)}{\lambda_{\min}(P)} \right) V, \quad (28)$$

For simplicity, we define

$$\gamma_1 = \frac{\lambda_{\min}(Q)}{\lambda_{\max}^{\frac{1}{2}}(P)}, \quad \gamma_2 = \frac{F\|q_1\|_2}{\lambda_{\min}^{\frac{1}{2}}(P)}, \quad \gamma_3 = \frac{\lambda_{\min}(\Omega_2)}{\lambda_{\max}(P)}, \quad \gamma_4 = \frac{\lambda_{\max}(Q)}{2\lambda_{\min}(P)}. \quad (29)$$

$\gamma_1, \gamma_2, \gamma_3, \gamma_4$ are all positive constants. Thus, equation (28) is simplified as,

$$\dot{V} \leq - (l(t)\gamma_1 - \gamma_2) V^{\frac{1}{2}} - \left(l(t)\gamma_3 - \frac{\dot{l}}{l(t)}\gamma_4 \right) V, \quad (30)$$

Since $\dot{l}(t) \geq 0$, such that the terms $l(t)\gamma_1 - \gamma_2$ and $l(t)\gamma_3 - \frac{\dot{l}}{l(t)}\gamma_4$ are positive in finite time, it follows from (30) that

$$\dot{V} \leq -c_1 V^{\frac{1}{2}} - c_2 V \quad (31)$$

where c_1, c_2 are positive constants. By the comparison principle [24] it follows that $V(\zeta)$, and therefore ζ converge to zero in finite time. Thus, Theorem 1 is proven. ■

It follows from Theorem 1 that when the sliding motion takes place $e_1 = 0, \dot{e}_1 = 0$. Thus, the output-error equivalent injection $\mu(e_1)$ can be obtained directly from equation (12),

$$\mu(e_1) = -\frac{u_1}{L}e_2 - \frac{u_2}{L}e_3 \quad (32)$$

Substitute (32) into the error system (13,14) that results the following reduced order system,

$$\begin{cases} \dot{e}_2 = k_1 \left(\frac{u_1}{L}e_2 + \frac{u_2}{L}e_3 \right), \\ \dot{e}_3 = k_2 \left(\frac{u_1}{L}e_2 + \frac{u_2}{L}e_3 \right). \end{cases} \quad (33)$$

Proposition 1. Consider the reduced order system (33) with the switching gains k_1, k_2 (17). Then, the trajectories of the dynamical error system (33) converge to zero exponentially if the following two conditions are satisfied [25]

- The exists a constant $\phi_M > 0$ such that for all $t \geq 0$, and all $u \in \mathcal{D}$, where $\mathcal{D} \in \mathbb{R}^2$ is a closed compact subset, $\|\Psi(t, u)\| \leq \phi_M$, where

$$\Psi(t, u) = \begin{bmatrix} \sqrt{\frac{k}{L}}u_1(t) & \sqrt{\frac{k}{L}}u_2(t) \end{bmatrix}^T \quad (34)$$

- There exists a constant $T_1, \mu > 0$ such that

$$\int_t^{t+T_1} \Psi(\tau, u) \Psi^T(\tau, u) d\tau \geq \mu I > 0, \quad \forall t \geq 0. \quad (35)$$

Proof: Define the vector $e_V^T = [e_2 \ e_3]$, substitute k_1, k_2 of (17) into the system (33), it follows that,

$$\dot{e}_V = -\frac{k}{L} \begin{bmatrix} u_1^2 & u_1 u_2 \\ u_1 u_2 & u_2^2 \end{bmatrix} e_V = -\Psi(\tau, u) \Psi^T(\tau, u) e_V, \quad (36)$$

Since the switch signals u is generated by a simple PWM, $\|\Psi(t, u)\| \leq \sqrt{\frac{k}{L}}\|u\| \leq \sqrt{2\frac{k}{L}}$ and T_1 can be chosen as one period of the switching sequence to verify the condition (35). Given that the conditions (34, 35) hold, it follows from [25] that the reduced order system (33) are exponentially stable. Thus, Proposition 1 is proven. ■

V. SIMULATION RESULTS

The performance of the proposed adaptive-gain SOSML observer has been evaluated in terms of the effectiveness and behavior through simulation. In order to highlight the improvement of the proposed strategy, the obtained results are compared with a Luenberger switched observer in [26]. Simulation parameters are shown in Table II. Furthermore, load resistance has been varied up to 50% to demonstrate the robustness of the proposed observer.

The system (8) is rewritten in a form convenient for designing the Luenberger switched observer [26],

$$\begin{cases} \dot{\hat{I}} = -\frac{R}{L}\hat{I} + \frac{E}{L}u_3 - \frac{\hat{V}_{c1}}{L}u_1 - \frac{\hat{V}_{c2}}{L}u_2 + \kappa_0 e_1, \\ \dot{\hat{V}_{c1}} = \frac{u_1}{c_1}I + (\kappa_1 u_1 + \kappa_3 u_2 + \kappa_5 u_3)e_1, \\ \dot{\hat{V}_{c2}} = \frac{u_2}{c_2}I + (\kappa_2 u_1 + \kappa_4 u_2 + \kappa_6 u_3)e_1. \end{cases} \quad (37)$$

TABLE II
MAIN PARAMETERS OF SIMULATION MODEL

System Parameters	Values
DC voltage(E)	150V
Capacitors(c_1, c_2)	40*10uF
Load resistance(R)	131Ω
Load Inductor(L)	10mH
The chopping frequency	5kHz
The sampling period	5us

The error dynamics of $e^T = [e_1 \ e_2 \ e_3]$ are given from equations (8) and (37),

$$\dot{e} = (\tilde{A}_0 + u_1 \tilde{A}_1 + u_2 \tilde{A}_2 + u_3 \tilde{A}_3)e \quad (38)$$

where $\tilde{A}_i = A_i - K_i C$, $i = 0, 1, 2, 3$, $K_0^T = (\kappa_0, 0, 0)$, $K_1^T = (0, \kappa_1, \kappa_2)$, $K_2^T = (0, \kappa_3, \kappa_4)$, $K_3^T = (0, \kappa_5, \kappa_6)$. The constant gains $\kappa_0, \kappa_1, \kappa_2, \kappa_3, \kappa_4, \kappa_5, \kappa_6$ are chosen such that there exists a positive matrix \tilde{P} which satisfies $\tilde{A}_i^T \tilde{P} + \tilde{P} \tilde{A}_i \leq 0$, for $i = 0, 1, 2, 3$. All the details of the parameters can be found in [26].

For simulation purpose, the initial values are chosen as,

$$V_{c_1}(0) = 0V, \quad V_{c_2}(0) = 0V, \quad \hat{V}_{c_1}(0) = 5V, \quad \hat{V}_{c_2}(0) = 10V.$$

the parameters of the adaptive SOSML algorithm (15,16) is chosen as $\lambda_0 = 2$, $\alpha_0 = 4$, $k_{\lambda_0} = 2.5$, $k_{\alpha_0} = 20$, $k = 6 \cdot 10^5$. The parameter of the switching gains (17) is chosen $\kappa = 20$. The inputs of the switches u are generated by a simple PWM with a chopping frequency 5kHz, the sampled period is 200kHz.

Figure 2 shows the estimations of the capacitor voltages V_{c_1}, V_{c_2} and its errors when the system is not affected by output noise and without load variation. Both the adaptive-gain SOSML observer and Luenberger switched observer can achieve desired performance.

The system output noise is taken into account in order to test the robustness of the proposed observers [7], which is shown in Figure 4. The estimations of the capacitor voltages V_{c_1}, V_{c_2} and its errors when the system is affected by the output noise and under load variation up to 50% are shown in Figure 3. As we can see from the figures, the proposed observers is rather robust and the effect of the noise is almost imperceptible. However, in the case of Luenberger switched observer, it seems more sensitive to the noise and load variation. From the work [27], we know that the SOSM observer works as a robust exact differentiator, for this reason we see better performance of the proposed observer compared with Luenberger switched observer. Figure 5 shows that the adaptive law of (15, 16) is effective under the condition of load variation.

VI. CONCLUSIONS

In this paper, a novel adaptive-gain SOSML observer is proposed for the multi-cell system which belongs to a class of hybrid systems. With the help of $Z(T_N)$ observability,

it enables to estimate the capacitor voltages under a certain condition of the input sequences, even the system does not satisfy the observability rank condition. That is, the system becomes observable in the sense of $Z(T_N)$ observability after several switching sequences. The robustness of the proposed observer and Luenberger switched observer was verified by the load resistance variation and output measurement noise influence. It was found that the adaptive-gain SOSML observer is more robust than the Luenberger switched observer. Two main advantages of the proposed method: 1) Only one parameter κ needs to be tuned; 2) There is no need a-priori requirement of the perturbation bounds.

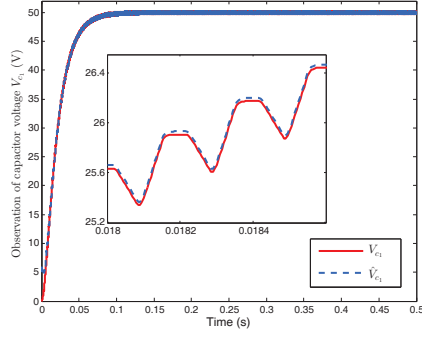
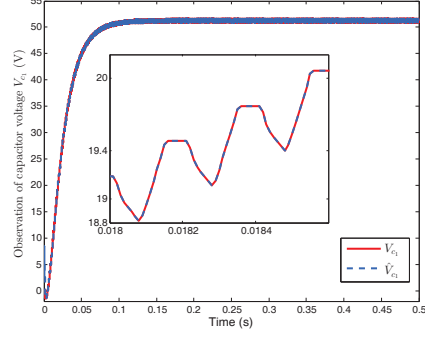
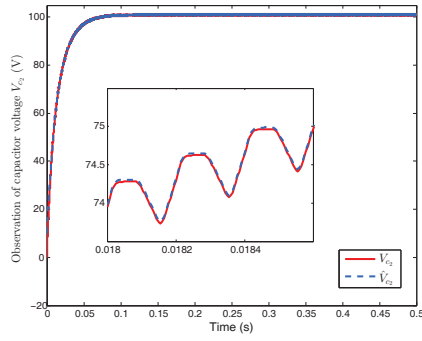
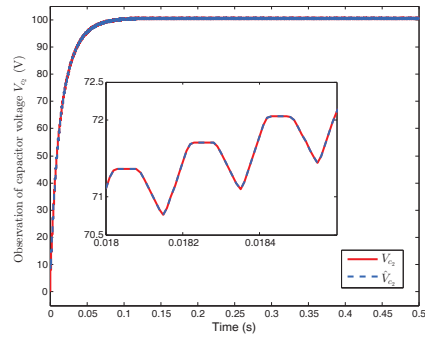
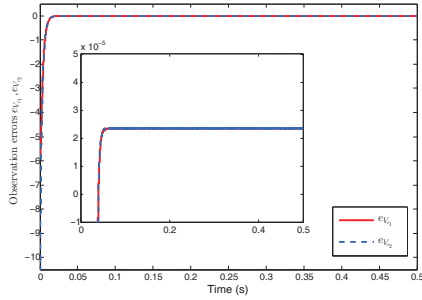
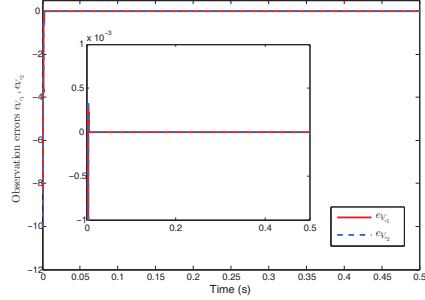
(a) Observation of V_{c1} (b) Observation of V_{c1} (c) Observation of V_{c2} (d) Observation of V_{c2} (e) Observation errors $e_{V_{c1}}, e_{V_{c2}}$ (f) Observation errors $e_{V_{c1}}, e_{V_{c2}}$

Fig. 2. Observation of capacitor voltage V_{c1}, V_{c2} and its errors in case of Adaptive-gain SOSML (2(a), 2(c), 2(e)) and Luenberger switched observer (2(b), 2(d), 2(f)) respectively when the system output is not affected by the noise and load variation

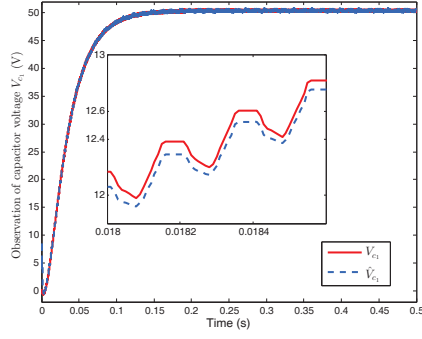
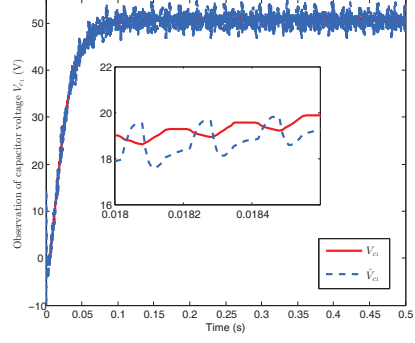
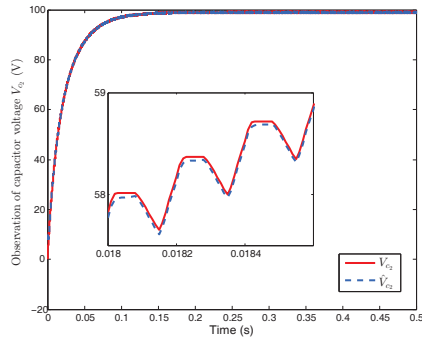
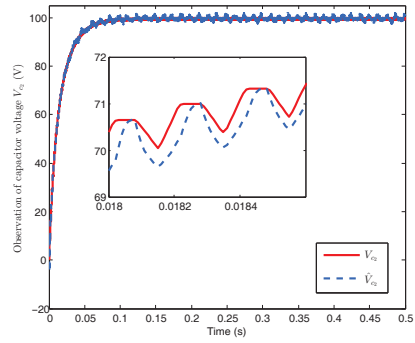
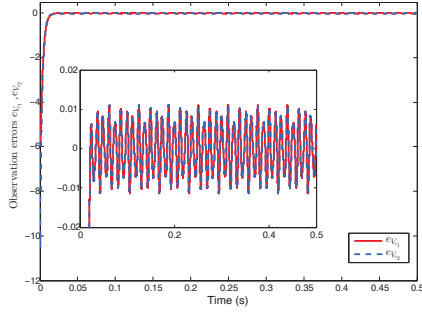
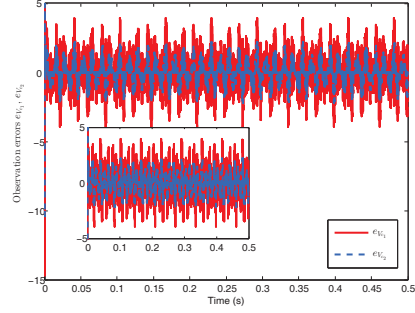
(a) Observation of V_{c1} (b) Observation of V_{c1} (c) Observation of V_{c2} (d) Observation of V_{c2} (e) Observation errors $e_{V_{c1}}, e_{V_{c2}}$ (f) Observation errors $e_{V_{c1}}, e_{V_{c2}}$

Fig. 3. Observation of capacitor voltage V_{c1}, V_{c2} and its errors in case of Adaptive-gain SOSML (3(a), 3(c), 3(e)) and Luenberger switched observer (3(b), 3(d), 3(f)) respectively when the system output is affected by the noise and load variation $\hat{R} = 1.5R$

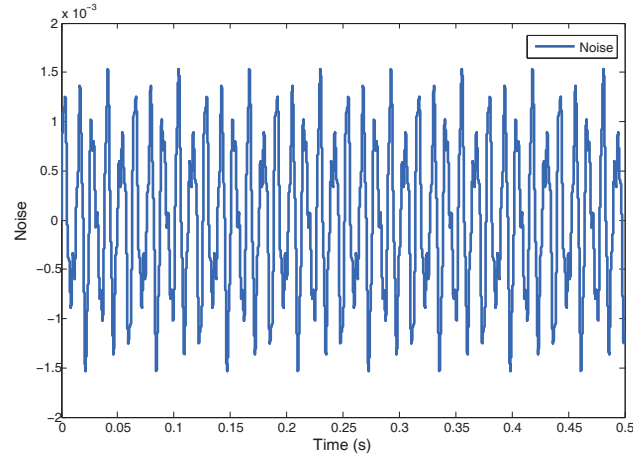


Fig. 4. Noise affect the system output

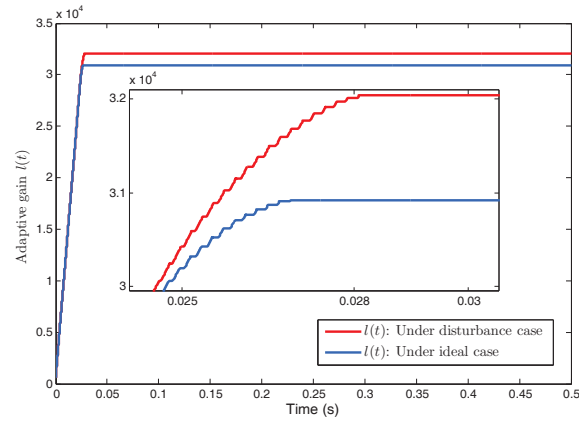


Fig. 5. Adaptive-law of $l(t)$ of the SOSML algorithm

REFERENCES

- [1] T. Meynard and H. Foch, "Multi-Level Conversion: High Voltage Choppers and Voltage-Source Inverters," in *23rd Annual Power Electronics Specialists Conference, 1992*. IEEE, 1992, pp. 397–403.
- [2] J. Rodriguez, J. Lai, and F. Peng, "Multilevel Inverters: a Survey of Topologies, Controls, and Applications," *IEEE Transactions on Industrial Electronics*, vol. 49, no. 4, pp. 724–738, 2002.
- [3] C. Rech and J. Pinheiro, "Hybrid Multilevel Converters: Unified Analysis and Design Considerations," *IEEE Transactions on Industrial Electronics*, vol. 54, no. 2, pp. 1092–1104, 2007.
- [4] D. Gerry, P. Wheeler, and J. Clare, "High-Voltage Multicellular Converters Applied to AC/AC Conversion," *International Journal of Electronics*, vol. 90, no. 11-12, pp. 751–762, 2003.

- [5] G. Gateau, M. Fadel, P. Maussion, R. Bensaid, and T. Meynard, "Multicell Converters: Active Control and Observation of Flying-Capacitor Voltages," *IEEE Transactions on Industrial Electronics*, vol. 49, no. 5, pp. 998–1008, 2002.
- [6] T. Meynard, M. Fadel, and N. Aouda, "Modeling of Multilevel Converters," *IEEE Transactions on Industrial Electronics*, vol. 44, no. 3, pp. 356–364, 1997.
- [7] F. Bejarano, M. Ghanes, and J.-P. Barbot, "Observability and Observer Design for Hybrid Multicell Choppers," *International Journal of Control*, vol. 83, no. 3, pp. 617–632, 2010.
- [8] M. Djemaï, K. Busawon, K. Benmansour, and A. Marouf, "High-Order Sliding Mode Control of a DC Motor Drive Via a Switched Controlled Multi-Cellular Converter," *International Journal of Systems Science*, vol. 42, no. 11, pp. 1869–1882, 2011.
- [9] M. Defoort, M. Djemaï, T. Floquet, and W. Perruquetti, "Robust Finite Time Observer Design for Multicellular Converters," *International Journal of Systems Science*, vol. 42, no. 11, pp. 1859–1868, 2011.
- [10] F. Defaÿ, A. Llor, and M. Fadel, "A Predictive Control With Flying Capacitor Balancing of a Multicell Active Power Filter," *IEEE Transactions on Industrial Electronics*, vol. 55, no. 9, pp. 3212–3220, 2008.
- [11] M. Bâja, D. Patino, H. Cormerais, P. Riedinger, and J. Buisson, "Hybrid Control of a Three-Level Three-Cell DC-DC Converter," in *American Control Conference (ACC), 2007*. IEEE, 2007, pp. 5458–5463.
- [12] P. Lezana, R. Aguilera, and D. Quevedo, "Model Predictive Control of an Asymmetric Flying Capacitor Converter," *IEEE Transactions on Industrial Electronics*, vol. 56, no. 6, pp. 1839–1846, 2009.
- [13] S. Meradi, K. Benmansour, K. Herizi, M. Tadjine, and M. Boucherit, "Sliding Mode and Fault Tolerant Control for Multicell Converter Four Quadrants," *Electric Power Systems Research*, vol. 95, no. 0, pp. 128–139, 2013. [Online]. Available: <http://www.sciencedirect.com/science/article/pii/S0378779612002672>
- [14] L. Amet, M. Ghanes, J.P. Barbot, "Direct Control Based on Sliding Mode Techniques for Multicell Serial Chopper," in *American Control Conference (ACC), 2011*, 29 2011-july 1 2011, pp. 751 –756.
- [15] G. Besançon, *Nonlinear Observers and Applications*. Springer Verlag, 2007, vol. 363.
- [16] R. Vidal, A. Chiuso, S. Soatto, and S. Sastry, "Observability of Linear Hybrid Systems," *Hybrid Systems: Computation and Control*, pp. 526–539, 2003.
- [17] M. Babaali and G. Pappas, "Observability of Switched Linear Systems in Continuous Time," *Hybrid systems: Computation and control*, pp. 103–117, 2005.
- [18] W. Kang, J. Barbot, and L. Xu, "On the Observability of Nonlinear and Switched Systems," *Emergent Problems in Nonlinear Systems and Control*, pp. 199–216, 2009.
- [19] M. Ghanes, F. Bejarano and J.P. Barbot, "On Sliding Mode and Adaptive Observers Design for Multicell Converter," in *American Control Conference (ACC), 2009*. IEEE, 2009, pp. 2134–2139.
- [20] J. Moreno and M. Osorio, "A Lyapunov Approach to Second-Order Sliding Mode Controllers and Observers," in *47th IEEE Conference on Decision and Control, CDC 2008*. IEEE, 2008, pp. 2856–2861.
- [21] W. Respondek, A. Pogromsky, and H. Nijmeijer, "Time Scaling for Observer Design with Linearizable Error Dynamics," *Automatica*, vol. 40, no. 2, pp. 277–285, 2004. [Online]. Available: <http://www.sciencedirect.com/science/article/pii/S0005109803002966>
- [22] B. McGrath and D. Holmes, "Analytical Modelling of Voltage Balance Dynamics for a Flying Capacitor Multilevel Converter," in *Power Electronics Specialists Conference, 2007. PESC, IEEE*, june 2007, pp. 1810–1816.
- [23] W. Perruquetti and J. Barbot, *Sliding Mode Control in Engineering*. CRC, 2002, vol. 11.
- [24] Hassan K. Khalil, *Nonlinear Systems*. Prentice hall New Jersey, 2007, vol. 3.
- [25] A. Lora and E. Panteley, "Uniform exponential stability of linear time-varying systems: revisited," *Systems & Control Letters*, vol. 47, no. 1, pp. 13–24, 2002. [Online]. Available: <http://www.sciencedirect.com/science/article/pii/S0167691102001652>
- [26] P. Riedinger, M. Sigalotti, and J. Daafouz, "On the Algebraic Characterization of Invariant Sets of Switched Linear Systems," *Automatica*, vol. 46, no. 6, pp. 1047–1052, 2010. [Online]. Available: <http://www.sciencedirect.com/science/article/pii/S0005109810001202>
- [27] A. Levant, "Robust Exact Differentiation Via Sliding Mode Technique," *Automatica*, vol. 34, no. 3, pp. 379–384, 1998.